Direct observation of a roaming intermediate and its dynamics

Grite L. Abma,[1] Michael A. Parkes,[2] Weronika O. Razmus,[3]

Yu Zhang,[4] Adam S. Wyatt,[4] Emma Springate,[4] Richard T. Chapman,[4]

Daniel A. Horke,[1*], Russell S. Minns[3*]

[1]Radboud University, Institute for Molecules and Materials,

Heijendaalseweg 135, 6525 AJ Nijmegen, The Netherlands

[2]Department of Chemistry, University College London, 20 Gordon Street, London

[3]School of Chemistry, University of Southampton,

Highfield, Southampton SO17 1BJ, UK

[4]Central Laser Facility, STFC Rutherford Appleton Laboratory,

Didcot, Oxfordshire OX11 0QX, UK

[*]To whom correspondence should be addressed;

DAH: d.horke@science.ru.nl, RSM: r.s.minns@soton.ac.uk.

(Dated: April 11, 2024)

Abstract

Chemical reactions are often characterised by their transition state, which defines the critical geometry the molecule must pass through to move from reactants to products. Roaming provides an alternative picture, where in a dissociation reaction the bond breaking is frustrated, and a loosely bound intermediate is formed. Following bond breaking the two partners are seen to roam around each other at distances of several Ångstroms, forming a loosely bound, and structurally ill-defined, intermediate that can subsequently lead to reactive or unreactive collisions. Here we present a direct and time-resolved experimental measurement of roaming. By measuring the photoelectron spectrum of UV excited acetaldehyde with a femtosecond extreme ultraviolet pulse, we captured spectral signatures of all of the key reactive structures including that of the roaming intermediate. This provided a direct experimental measurement of the roaming process and allowed us to identify the timescales by which the roaming intermediate is formed and removed, and the electronic potential surfaces upon which roaming proceeds.

I.   Introduction

The traditional view of a chemical reaction relies on transition state theory, where specific structures act as bottlenecks through which reactants must pass to form products. Over the course of the past 15 years a new type of photodissociation reaction mechanism, termed 'roaming', has offered an alternative to this view and is thought to compete with conventional transition state driven dynamics.[1–6] This roaming pathway can occur when, en route to dissociation, a shallow plateau in the potential energy surface is encountered, leading to the formation of a quasi-bound complex of two fragments.

Roaming was first discovered in formaldehyde, in which an intermediate is formed by a hydrogen atom roaming around a HCO radical.[1] Since this first observation, the roaming pathway has been experimentally shown in several systems and is thought to be nearly ubiquitous in photodissociation reactions.[4,7,8] Direct experimental observation of the roaming intermediates is however challenging, meaning that roaming processes have largely been identified through the detailed analysis of the energy partitioning detected in the final reaction products and correlations in the usually bimodal internal energy distribution of the fragments has been used as evidence of roaming processes.[2,3,5,9]

The challenge to experiment is that the characteristics of roaming intermediates place extreme constraints on the measurement processes used. By its very nature, the occurrence of roaming produces a molecular complex that has an impossible to define geometry as the reaction intermediate. The roaming partners can take on a wide range of structures defined by a broad plateau on the potential energy surface. The typically rapid formation of the intermediate and subsequent slow decay necessitates measurements on timescales covering many orders of magnitude, potentially from femtoseconds to nanoseconds. These characteristics provide a demanding backdrop to experiment and theory alike. Accurate theoretical descriptions of the roaming wavepacket are difficult to perform, while the identification of specific structural or spectral probes are challenging to experiments.

Experimental probes that are sensitive to all aspects of the roaming dynamics are needed, ideally capturing the formation and decay of the roaming intermediate, as well as the final products formed. To the best of our knowledge, the first experimental observation of a roaming intermediate was only recently reported. Utilising a time-resolved Coulomb explosion imaging measurement with coincident detection of multiple fragment ions, the authors were

2

able to identify a signature of the first step in the roaming process in formaldehyde, as well as the formation of the intermediate complex on a timescale of a few hundred femtoseconds.[6] However, a full time-resolved measurement of roaming dynamics, and of the eventual fate of the intermediate, has so far not been reported.

Herein we report on the direct and time-resolved observation of the formation and subsequent decay of the roaming intermediate in the photodissociation of acetaldehyde (CH_3CHO). Here UV absorption leads to the carbon-carbon bond breaking and the formation of CH_3 and HCO radicals. The radicals begin to separate and can either follow a pathway that is well described by conventional transition state theory and rapidly leads to the separation of the two radical fragments, or a roaming pathway where the two fragments are seen to remain in relative close proximity (at $C-C$ distances of 3-4 Å[4]) for an extended period of time. For the molecules that follow the roaming pathway, the two radicals explore a wide range of configurations before reaching one that allows for reaction of the two fragments, forming CH_4 and CO, or dissociation leading to the relatively delayed formation of the radical products. The roaming channel in this photodissociation has been studied by various groups both theoretically[10–12] and experimentally[3,9,13–19] and at a vast range of dissociation energies from $\sim$220–330 nm.[17] The primary experimental observable in all these studies was the energy distribution of final radical (HCO, CH_3) or molecular (CO, CH_4) products, meaning a direct observation of the roaming intermediate, and its formation pathway, has so far remained difficult to measure. Existing time-resolved studies lack the necessary temporal resolution to observe the crucial first electronic dynamics following photoexcitation.[14,15] Here we study the ultrafast dynamics following excitation of acetaldehyde at 262 nm (4.7 eV), populating the first electronically excited state (S_1) via a $\pi^* \leftarrow n$ transition.[20] At this excitation energy the dissociation mechanism is not well understood, with some studies invoking intersystem crossing to lower lying triplet states as a potential relaxation pathway,[14,19] while others suggest that at these pump wavelengths the available energy is sufficient to overcome a barrier on the S_1 surface, leading to internal conversion via a conical intersection with the singlet ground state S_0.[10,11,16–18] Following internal conversion the system can either directly dissociate, or it can lead to roaming by exploring a wide plateau on the potential surface, eventually leading to both radical and molecular dissociation channels. To directly observe the formation and subsequent destruction of the roaming intermediate, we present here a photoelectron spectroscopy experiment which utilizes a femtosecond extreme ultraviolet

[93] (XUV) probe pulse.[21] The sensitivity of photoelectron spectroscopy to changes in the bonding

[94] character, combined with the high energy of the probe, allowed us to monitor all aspects

[95] of a roaming reaction.[22,23] The measurements captured spectroscopic signals that are only

[96] consistent with the formation and removal of roaming intermediates, as well as the formation

[97] of the HCO radical product via direct and roaming reaction pathways. The experimental

[98] data is supported by *ab-initio* calculations of the potential energy surfaces and simulated

[99] photoelectron spectra, which allows us to identify the electronic state upon which roaming

[100] proceeds.

II. Results and Discussion

[102]   Resulting photoelectron spectra are shown in Figure 1. In panel **a** we show characteristic

[103] photoelectron spectra at selected pump-probe delays. With pump and probe pulses temporally

[104] overlapped (t_0, red trace) we observe two broad peaks centred around binding energies of

[105] 5.5 eV and 8.5 eV. These correspond to ionisation of the initially excited state of the bound

[106] CH_3CHO molecule into the ground (D_0) and first electronically excited (D_1) state of the ion,

[107] respectively. These features are very short lived, and by 500 fs (purple trace) we observe only

[108] a very broad feature from around 6.0 eV to at least 9.0 eV binding energy, beyond this energy

[109] any signals are obscured by the direct ionisation of ground state acetaldehyde, as further

[110] discussed in the supplementary information. Going towards even longer delays (600 ps, green

[111] trace) this broad feature has narrowed and shifted towards higher binding energies, and now

[112] corresponds to final reaction products, in this case the formation of the HCO radical, as

[113] further discussed below.

[114]   In Figure 1**b** we show the full time-resolved photoelectron spectrum, note the mixed

[115] linear-logarithmic scale on the time delay (y) axis. The full spectrum highlights the very

[116] short lived nature of the initially excited state, and the formation of a broad peak within a

[117] few hundred femtoseconds. On longer timescales of hundreds of picoseconds this peak is seen

[118] to decrease in intensity on the low binding energy side.

[119]   To extract dynamic information we integrate the time-resolved spectrum over selected

[120] binding energy slices, Figure 2. The green trace in panel **a** shows the dynamics in the

[121] 5.2–5.8 eV binding energy region, corresponding to the initially excited state in acetaldehyde.

[122] A rapid exponential decay with a time constant of around 50 fs is observed, which we assign to
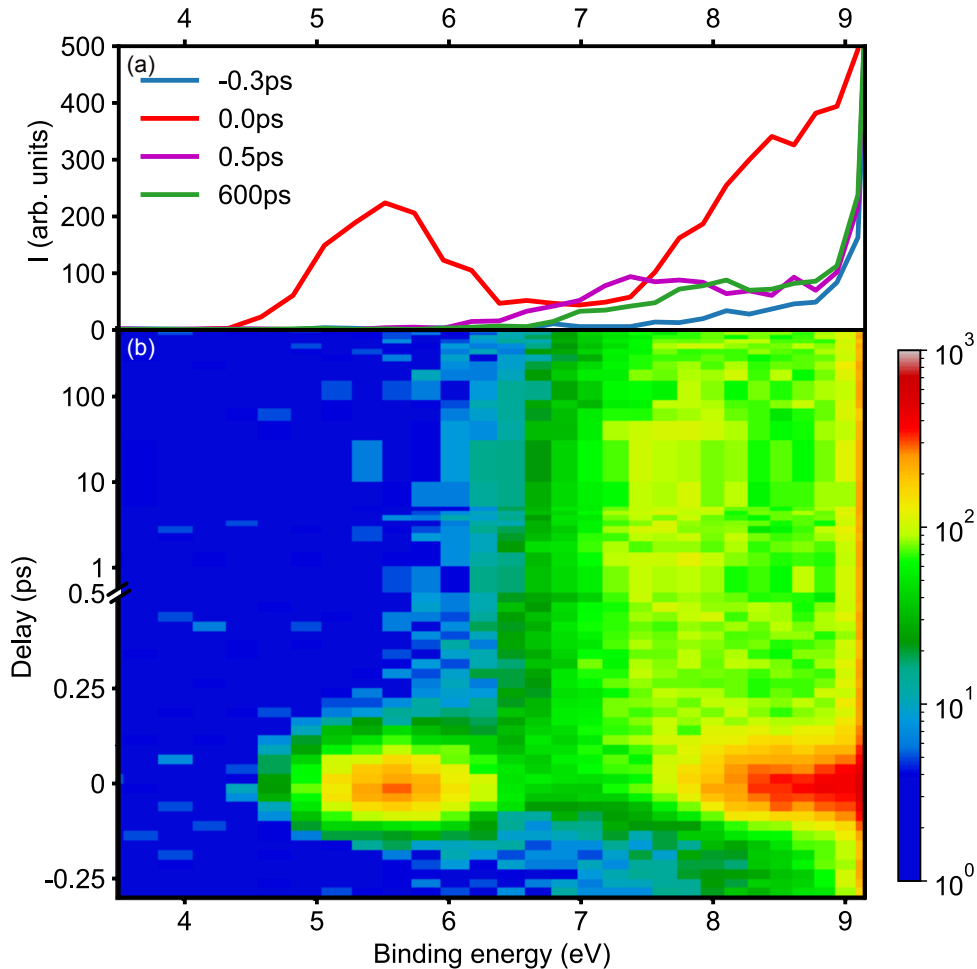
4

FIG. 1. Time-resolved photoelectron spectra of acetaldehyde following excitation at 262 nm and ionization at 56 nm (22.3 eV). a) Selected spectra at different pump-probe delays, before t_0(blue), at t_0(red), at 500 fs (purple) and at long delays of 600 ps (green). b) Surface plot showing the time evolution of the photoelectron spectra, note the mixed linear-logarithmic time delay (y) axis, which is linear up to 0.5 ps, and logarithmic thereafter.

the rapid depopulation of the initially excited S_1 state. The blue traces in Figure 2**a**–**b** show the binding energy region of 6.7–7.3 eV. Following a fast rise, a slow decay on a timescale of a few hundred picoseconds is observed, until a plateau of around half the intensity is reached. This behaviour clearly indicates the existence of multiple overlapping contributions to the photoelectron spectrum, belonging to a transient state decaying on the 100s of picosecond timescale, and a (much) longer lived contribution likely from a reaction product. In order to deconvolve these we perform a global 2D fit to the entire time-resolved photoelectron
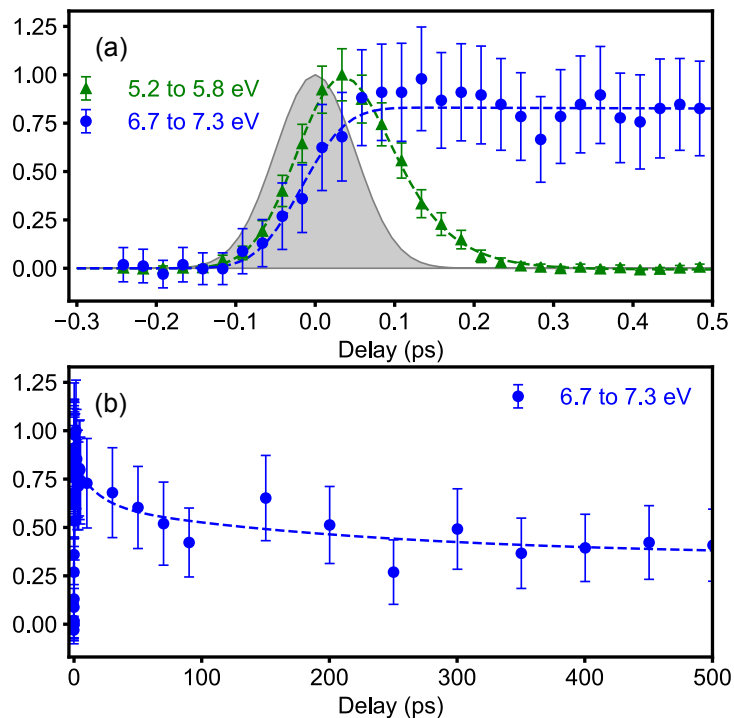
FIG. 2. Time evolution of the observed photoelectron signal in selected energy regions on short (a) and long (b) timescales. Grey shading in (a) corresponds to the instrument response function as discussed in the experimental details section of the SI.

spectrum to extract so-called decay-associated spectra (DAS), which represent the spectral contribution to each underlying dynamical process.[24–26] We require a total of 3 separate processes, each with its own associated lifetime, to accurately represent the data.

The resultant DAS are plotted in Figure 3, and have associated time constants of 50 fs, >2.5 ns and 190 ps in panels **a**–**c**, respectively. At early times the dynamics are dominated by the spectral contribution shown in the top panel of Figure 3. The broad peaks correlate well with the expected binding energies for ionisation from the Franck-Condon geometry of the initially excited S_1 state. These peaks have an associated time constant of approximately 50 fs, meaning this is an extremely short lived configuration of the molecule.

In Figure 3**b** we show the spectral component that has an associated lifetime of >2.5 ns. This is much longer than the timescale of our experiment and hence can be considered an 'infinite lifetime', such that on the timescale measured the intensity remains unchanged and this corresponds to one of the products of the reaction. Based on the known reaction products and their ionisation energies, (CH_3 9.84 eV , HCO 8.1 eV, CH_4 12.61 eV, CO 14.01 eV)[27] we
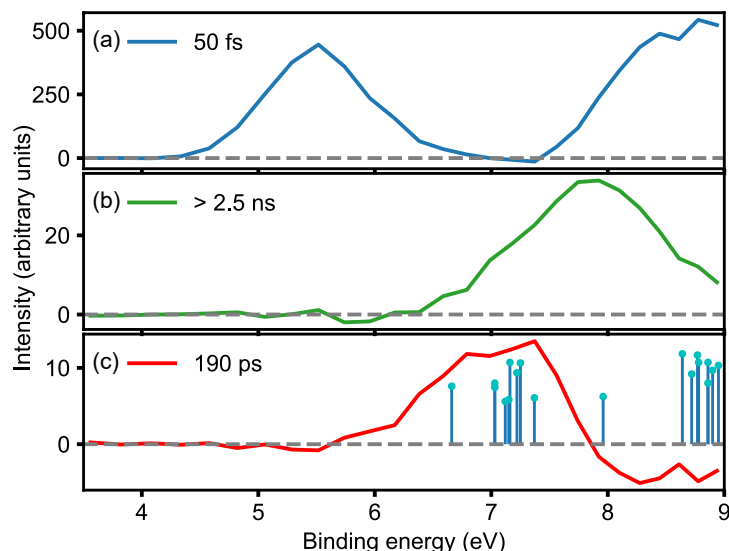
FIG. 3. Decay associated spectra extracted from the experimental data in Figure 1. Three time constants of 50 fs (a), >2.5 ns (b) and 190 ps (c) are required to accurately represent the data. In panel (c) calculated binding energies following ionisation of the roaming intermediate in various geometries on the S_0 state are indicated as sticks, with the length corresponding to the relative cross-section.

assign this feature to the rapid formation of HCO, occurring within the first 100 fs after excitation. As the HCO fragment can only be formed on the electronic ground state, the appearance of this product also indicates that the internal conversion from S_1 to S_0 occurs on this ultrafast timescale.

The lower panel in Figure 3 shows a more complex spectrum, including regions of positive and negative amplitude, with an associated time constant of 190±10 ps. The uncertainty corresponds to a statistical 2σ standard error extracted from the DAS fitting, further details are given in the supplementary information. In DAS, regions of positive amplitude relate to spectral features that decay on the associated timescale (as seen in Figure 3**a**–**b**), whilst negative amplitudes relate to spectral features that increase in intensity on that timescale. The observation of both positive and negative amplitudes within the DAS is therefore a direct sign for the flow of population from one region of the spectrum, where positive amplitude is observed, to regions of the spectrum with a negative amplitude. Figure 3**c** therefore clearly shows the decay of a species with binding energies in the range 5.3–7.6 eV into a new species with higher binding energies on a timescale of 190 ps. At these higher binding energies

7

the signal strongly overlaps with the observed HCO peak (Figure 3b), indicating that we are producing additional HCO fragments over this much longer time scale, in addition to those produced from the rapid initial dissociation. The observed feature in the 5.3–7.6 eV range therefore corresponds to a reactive intermediate, formed within the first few hundred femtosecond after excitation, and decaying on a 190 ps timescale to yield (as one product) the HCO radical. We therefore assign this transient species to the roaming intermediate $CH_3 \cdots HCO$. The observed binding energy is indicative of an intermediate structure between a bound CH_3CHO and the radical product HCO, suggesting we are monitoring a range of structures associated with the weakly bound roaming intermediate. The observed rapid appearance of the intermediate within the first few hundred femtoseconds agrees well with recent observations in formaldehyde.[6]

Previous measurements have suggested the involvement of intersystem crossing (ISC) to the triplet states ([18,28–30]), which could also explain the observation of a photoelectron peak at these intermediate energies. We find this unlikely in the present situation due to the temporal characteristics of the spectral changes observed. For a molecule like acetaldehyde, which contains no heavy atoms, such rapid (sub 100 fs) and efficient ISC into the triplet manifold is extremely unlikely. The spin-orbit (SO) coupling matrix-element that facilitates ISC between S_1 and S_0 is approximately 10 cm^{-1}.[31] This means direct transfer from S_1 to T_1 on the measured lifetime of the S_1 state can be ruled out. Subsequent transfer from S_0 to T_1 is theoretically possible and has a larger associated SO-coupling of approximately 70 cm^{-1}. This process is energetically less favourable and would involve transfer onto a state with higher potential energy. The fact that the photoelectron band is formed extremely rapidly but subsequently remains unchanged indicates that there are no electronic structure changes on the timescale of the measurement. We therefore suggest that at the 262 nm pump wavelength used here, we excite into S_1 state above the barrier to the S_1/S_0 conical intersection.[10,11,16–18] Excitation above the barrier leads to rapid internal conversion to S_0 and the subsequent role of the triplet states is therefore negligibly small. We note that this assignment agrees with that suggested in previous experimental and theoretical studies.[17,32] At longer wavelengths, where the barrier on S_1 cannot be overcome, transitions to T_1 will become important and play a significant role in the reaction, as shown by a large number of studies performed at wavelengths longer than 300 nm.[9,18,33]

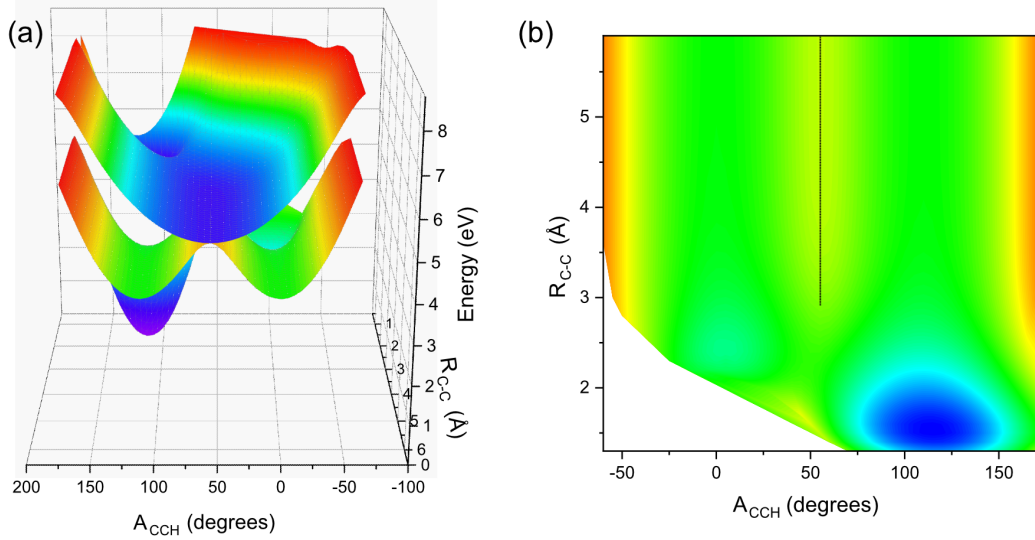In order to support our assignments, and to understand where on the potential energy

8

FIG. 4. Calculated potential energy surfaces of acetaldehyde. (a) Projection of the S_1 and S_0 surfaces along the C-C bond length and CCH bond angle coordinates. (b) Contour plot of the S_0 ground state surface, the dashed line indicated a conical intersection seam with the S_1 state.

surface roaming takes place, we calculated the coupled potential energy surfaces important to the dynamics, technical details are given in the supporting information. The acetaldehyde potential energy surface was explored at a range of $C-C$ bond lengths and $C-C-H$ bond angles. A projection of the initially excited S_1 and ground state S_0 surfaces are plotted in Figure 4**a**, with panel **b** showing a contour projection of the S_1 surface. The figure shows an extended crossing (points of degeneracy) between the two surfaces at a $C-C-H$ angle of 50° with $C-C$ bond lengths ~~of~~ greater than 2.5 Å(indicated by the dashed line in Figure 4**b**). Efficient population transfer is facilitated at these crossing points (conical intersection seam) allowing for rapid re-population of the electronic ground state. Surrounding this crossing associated with the conical intersection is a broad and flat plateau extending over a wide range of angles and bond lengths. We note that within the figure we can only provide a limited projection of the full potential energy surface (which would contain 15 dimensions) and this plateau extends over a much wider range of geometries than can be plotted within a single projection.

We have performed full quantum trajectory simulations covering the first 100 fs to confirm that ultrafast internal conversion is viable, see SI for details. The calculated electronic state populations show a rapid transfer from S_1 to S_0 occurring within 20 fs. This is in line with the

9

50 fs time constant observed experimentally for the decay of the initially excited state, and confirms our assignment of ultrafast internal conversion as the primary step in the dynamics.

While we cannot perform trajectory simulation for the full time frame of the experiment, the calculated ground and excited state potential energy surfaces provide us with a landscape upon which we can obtain theoretical photoelectron spectra for a variety of geometries associated with the initially excited Franck-Condon geometry, the dissociated fragments and the roaming intermediate. The geometries chosen for calculation of the roaming signal were based on the positions of the conventional and roaming transition state as reported by Bowman.[34] Fixed and relaxed geometry potential energy scans were then performed around these starting points and representative structures from these scans were taken forward for calculation of their photoelectron spectrum. Full details on the calculations can be found in the SI as we limit the presentation here to the calculated photoelectron energies for ionisation of the roaming intermediate on the ground electronic state. Calculated energies and relative cross-sections for various geometries on the broad plateau region are shown in Figure 3c, overlaid with the experimental photoelectron spectrum assigned to the roaming intermediate. The calculations show that a broad range of binding energies are possible, correlating with the 'floppy' structure of the molecule and the large regions of the potential energy surface explored. Importantly, several calculated photoelectron energies agree remarkably well with the feature assigned to the roaming intermediate, in the range of ∼6–8 eV binding energy, giving us confidence in the assignment of this feature to the roaming intermediate. A further cluster of expected photoelectron peaks is towards higher binding energies of > 8 eV. Experimentally, this roaming signal would overlap with the signal associated with the HCO product formation. As such, the amplitude observed in the DAS in this region between 8.5-9 eV would depend on the relative populations and cross-sections of the two contributions, as the roaming component would provide a positive amplitude and the HCO component a negative amplitude.

The combined experimental and theoretical results lead to the following picture of the dynamics. Absorption of a UV photon leads to population of the S_1 excited state. Here, the C−C bond distance increases en route to a conical intersection, where there is efficient population transfer *via* a conical intersection to the S_0 ground state,[10,16–18] the extremely fast timescale rules out any intersystem crossing into the triplet state. Once in the ground state a subset of the initially excited molecules continues along the dissociation path leading

10

to the rapid (50 fs) formation of the CH_3 and HCO fragments. The remaining quasi-bound population is associated with roaming dynamics of the CH_3 and HCO fragments, which explores a range of structures on the electronic ground state, which potentially include those associated with the various ground state minima. This roaming intermediate decays with a time constant of 190 ps and we observe the concomitant formation of additional free HCO fragments on this timescale. We note that other roaming channels, involving a roaming hydrogen atom, could contribute to the signal and that the formation of other products, such as CH_4+CO formed via reaction with the roaming HCO, or reformation of a vibrationally hot ground state molecule, could also contribute to the effective lifetime measured. Detection of the CH_4+CO fragments is in principle also possible in the experiment due to the high probe-energy used, however, the ionisation potentials of these species mean they strongly overlap with the background associated with ionisation of ground state CH_3CHO. As we wish to stay in the regime where single photon excitation is dominant, we are limited to a relatively low excited state population and yield of products, this mean we cannot extract reliable signal for these fragments.

Recent picosecond resolution action spectroscopy measurements of the products obtained following UV excitation suggest a much more complex set of electronic state transitions.[14,19] The experiments were performed at a similar, albeit slight lower pump energy (267 nm compared with 262 nm) which may explain the discrepancy. These action spectroscopy measurements suggested that the S_1 lifetime was on the order of 100's ps, with complex excited state dynamics over multiple electronic states required to explain the observation. We note that the evidence for the mechanisms is indirect, while our direct measurements capture the initial electronic state dynamics and ensure that processes exclusively associated with single photon excitation are observed. The increased time resolution also shows the S_1 lifetime at our pump wavelength is less than 100 fs and leads to a relatively straightforward explanation of the dynamics.

III. Conclusion

The sensitivity of our XUV photoelectron spectroscopy probe allowed us to monitor the key geometric and electronic structure changes associated with roaming dynamics. We directly observed the formation of the roaming intermediate on an ultrafast (<100 fs) timescale.

Detailed analysis of the resulting photoelectron spectrum and comparison to quantum chemical calculations allow us to show that roaming occurs on the electronic ground state, and that the eventual breakdown of the roaming intermediate occurs on a 190 picoseconds timescale. These experiments employing global probes with ultrafast time-resolution offer the possibility for detailed and direct insight into molecular roaming pathways, and to quantify the importance and prevalence of roaming processes in photochemistry.

IV. Supporting Information

Experimental details and description of data analysis procedures. Computational details and supporting calculations.

Acknowledgements

References

[1] Townsend, D.; Lahankar, S. A.; Lee, S. K.; Chambreau, S. D.; Suits, A. G.; Zhang, X.; Rheinecker, J.; Harding, L. B.; Bowman, J. M. The Roaming Atom: Straying from the Reaction Path in Formaldehyde Decomposition. *Science* **2004**, *306*, 1158–1161.

12

[2] Grubb, M. P.; Warter, M. L.; Xiao, H.; Maeda, S.; Morokuma, K.; North, S. W. No Straight Path: Roaming in Both Ground- and Excited-State Photolytic Channels of $NO_3 \rightarrow NO + O_2$. *Science* **2012**, *335*, 1075–1078.

[3] Heazlewood, B. R.; Jordan, M. J. T.; Kable, S. H.; Selby, T. M.; Osborn, D. L.; Shepler, B. C.; Braams, B. J.; Bowman, J. M. Roaming Is the Dominant Mechanism for Molecular Products in Acetaldehyde Photodissociation. *Proc. Natl. Acad. Sci. U.S.A.* **2008**, *105*, 12719–12724.

[4] Suits, A. G. Roaming Reactions and Dynamics in the van Der Waals Region. *Annu. Rev. Phys. Chem.* **2020**, *71*, 77–100.

[5] Quinn, M. S.; Nauta, K.; Jordan, M. J. T.; Bowman, J. M.; Houston, P. L.; Kable, S. H. Rotational Resonances in the H_2CO Roaming Reaction Are Revealed by Detailed Correlations. *Science* **2020**, *369*, 1592–1596.

[6] Endo, T. et al. Capturing Roaming Molecular Fragments in Real Time. *Science* **2020**, *370*, 1072–1077.

[7] Bowman, J. M.; Suits, A. G. Roaming Reactions: The Third Way. *Physics Today* **2011**, *64*, 33–37.

[8] Bowman, J. M.; Houston, P. L. Theories and Simulations of Roaming. *Chem. Soc. Rev.* **2017**, *46*, 7615–7624.

[9] Houston, P. L.; Kable, S. H. Photodissociation of Acetaldehyde as a Second Example of the Roaming Mechanism. *Proc. Natl. Acad. Sci. U.S.A.* **2006**, *103*, 16079–16082.

[10] Gherman, B. F.; Friesner, R. A.; Wong, T.-H.; Min, Z.; Bersohn, R. Photodissociation of Acetaldehyde: The CH_4+CO Channel. *J. Chem. Phys.* **2001**, *114*, 6128–6133.

[11] Shepler, B. C.; Braams, B. J.; Bowman, J. M. "Roaming" Dynamics in CH_3CHO Photodissociation Revealed on a Global Potential Energy Surface. *J. Phys. Chem. A* **2008**, *112*, 9344–9351.

[12] Harding, L. B.; Georgievskii, Y.; Klippenstein, S. J. Roaming Radical Kinetics in the Decomposition of Acetaldehyde. *J. Phys. Chem. A* **2010**, *114*, 765–777.

[13] Lee, K. L. K.; Quinn, M. S.; Maccarone, A. T.; Nauta, K.; Houston, P. L.; Reid, S. A.; Jordan, M. J. T.; Kable, S. H. Two Roaming Pathways in the Photolysis of CH_3CHO between 328 and 308 Nm. *Chem. Sci.* **2014**, *5*, 4633–4638.

[14] Yang, C.-H.; Bhattacharyya, S.; Liu, L.; Fang, W.-h.; Liu, K. Real-Time Tracking of the Entangled Pathways in the Multichannel Photodissociation of Acetaldehyde. *Chem. Sci.* **2020**,

327   *11*, 6423–6430.

[15] Toulson, B. W.; Kapnas, K. M.; Fishman, D. A.; Murray, C. Competing Pathways in the Near-UV Photochemistry of Acetaldehyde. *Phys. Chem. Chem. Phys.* **2017**, *19*, 14276–14288.

[16] Rubio-Lago, L.; Amaral, G. A.; Arregui, A.; Izquierdo, J. G.; Wang, F.; Zaouris, D.; Kitsopoulos, T. N.; Bañares, L. Slice Imaging of the Photodissociation of Acetaldehyde at 248 Nm. Evidence of a Roaming Mechanism. *Phys. Chem. Chem. Phys.* **2007**, *9*, 6123.

[17] Rubio-Lago, L.; Amaral, G. A.; Arregui, A.; González-Vázquez, J.; Bañares, L. Imaging the Molecular Channel in Acetaldehyde Photodissociation: Roaming and Transition State Mechanisms. *Phys. Chem. Chem. Phys.* **2012**, *14*, 6067.

[18] Heazlewood, B. R.; Rowling, S. J.; Maccarone, A. T.; Jordan, M. J. T.; Kable, S. H. Photochemical Formation of HCO and CH_3 on the Ground S0 (A1′) State of CH3CHO. *J. Chem. Phys.* **2009**, *130*, 054310.

[19] Yang, C.-H.; Bhattacharyya, S.; Liu, K. Time-Resolved Pair-Correlated Imaging of the Photodissociation of Acetaldehyde at 267 Nm: Pathway Partitioning. *J. Phys. Chem. A* **2021**, *125*, 6450–6460.

[20] Limão-Vieira, P.; Eden, S.; Mason, N.; Hoffmann, S. Electronic State Spectroscopy of Acetaldehyde, CH_3CHO, by High-Resolution VUV Photo-Absorption. *Chem. Phys. Lett.* **2003**, *376*, 737–747.

[21] Smith, A. D.; Warne, E. M.; Bellshaw, D.; Horke, D. A.; Tudorovskya, M.; Springate, E.; Jones, A. J. H.; Cacho, C.; Chapman, R. T.; Kirrander, A.; Minns, R. S. Mapping the Complete Reaction Path of a Complex Photochemical Reaction. *Phys. Rev. Lett.* **2018**, *120*, 183003.

[22] Hockett, P.; Bisgaard, C. Z.; Clarkin, O. J.; Stolow, A. Time-Resolved Imaging of Purely Valence-Electron Dynamics during a Chemical Reaction. *Nat. Physics* **2011**, *7*, 612–615.

[23] Schuurman, M. S.; Blanchet, V. Time-Resolved Photoelectron Spectroscopy: The Continuing Evolution of a Mature Technique. *Phys. Chem. Chem. Phys.* **2022**, *24*, 20012–20024.

[24] Bisgaard, C. Z.; Clarkin, O. J.; Wu, G.; Lee, A. M. D.; Geßner, O.; Hayden, C. C.; Stolow, A. Time-Resolved Molecular Frame Dynamics of Fixed-in-Space CS_2 Molecules. *Science* **2009**, *323*, 1464–1468.

[25] Satzger, H.; Townsend, D.; Zgierski, M. Z.; Patchkovskii, S.; Ullrich, S.; Stolow, A. Primary processes underlying the photostability of isolated DNA bases: Adenine. *Proceedings of the National Academy of Sciences* **2006**, *103*, 10196–10201.

14

[26] Chatterley, A. S.; West, C. W.; Stavros, V. G.; Verlet, J. R. R. Time-resolved photoelectron imaging of the isolated deprotonated nucleotides. *Chem. Sci.* **2014**, *5*, 3963–3975.

[27] Lias, S. G. In *NIST Chemistry WebBook, NIST Standard Reference Database Number 69*; Linstrom, P. J., Mallard, W. G., Eds.; National Institute of Standards and Technology: Gaithersburg , MD, 2022.

[28] Cruse, H. A.; Softley, T. P. Velocity-Map Imaging Study of the Photodissociation of Acetaldehyde. *J. Chem. Phys.* **2005**, *122*, 124303.

[29] Amaral, G. A.; Arregui, A.; Rubio-Lago, L.; Rodríguez, J. D.; Bañares, L. Imaging the radical channel in acetaldehyde photodissociation: Competing mechanisms at energies close to the triplet exit barrier. *The Journal of Chemical Physics* **2010**, *133*, 064303.

[30] Thompson, K. C.; Crittenden, D. L.; Kable, S. H.; Jordan, M. J. T. A classical trajectory study of the photodissociation of T1 acetaldehyde: The transition from impulsive to statistical dynamics. *The Journal of Chemical Physics* **2006**, *124*, 044302.

[31] Fu, B.; Han, Y.; Bowman, J. M. Three-state surface hopping calculations of acetaldehyde photodissociation to CH_3 + HCO on ab initio potential surfaces. *Faraday Discuss.* **2012**, *157*, 27–39.

[32] Chen, S.; Fang, W.-H. Insights into photodissociation dynamics of acetaldehyde from ab initio calculations and molecular dynamics simulations. *The Journal of Chemical Physics* **2009**, *131*, 054306.

[33] Li, H.-K.; Tsai, P.-Y.; Hung, K.-C.; Kasai, T.; Lin, K.-C. Communication: Photodissociation of CH_3CHO at 308 Nm: Observation of H-roaming, CH_3-Roaming, and Transition State Pathways Together along the Ground State Surface. *J. Chem. Phys.* **2015**, *142*, 041101.

[34] Shepler, B. C.; Han, Y.; Bowman, J. M. Are Roaming and Conventional Saddle Points for H_2CO and CH_3CHO Dissociation to Molecular Products Isolated from Each Other? *The Journal of Physical Chemistry Letters* **2011**, *2*, 834–838.
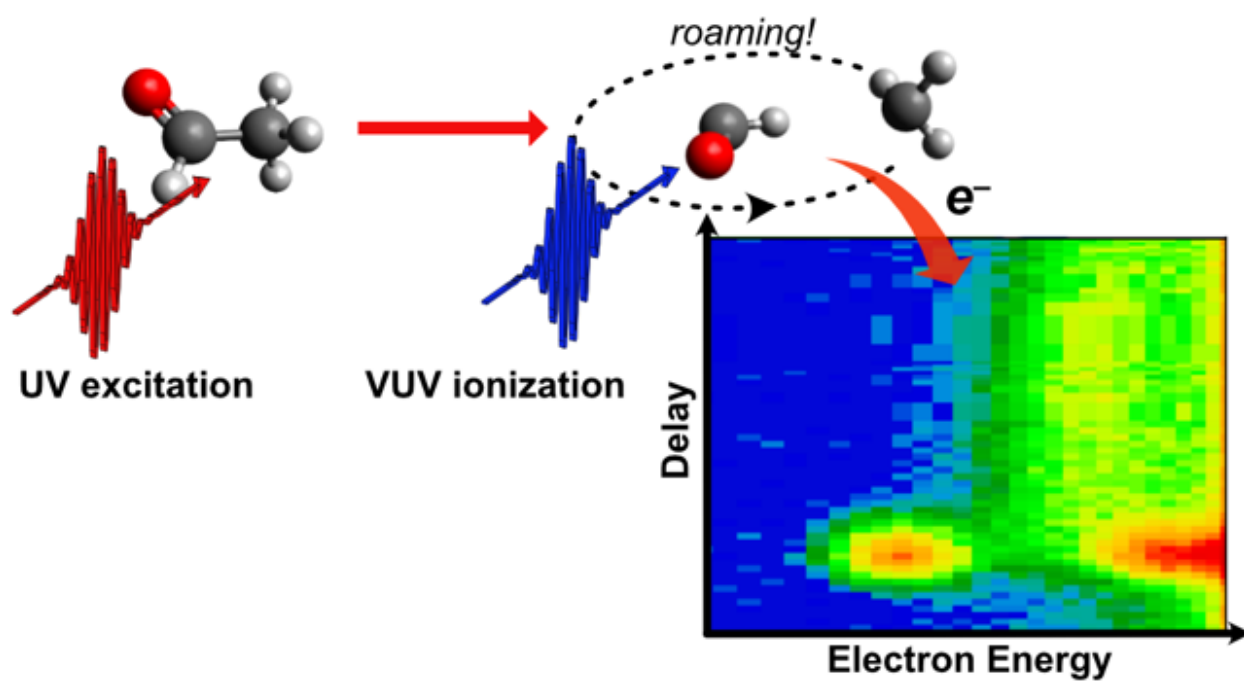
FIG. 5. TOC Graphic